Electronic Supplementary Material (ESI) for Nanoscale.


# Mechanically robust, UV screener core-double-shell nanostructures provide enhanced shielding for EM radiations over wide angle of incidence

Yudhajit Bhattacharjee, Sambit Bapari and Suryasarathi Bose *

[a] Department of Materials Engineering, Indian Institute of Science, Bangalore – 560012, India

*Author to whom all the correspondence should be addressed: sbose@iisc.ac.in

**Table of Content:**
**Page No.**

## *Mechanical testing of thin films using DIC*

Tensile samples of polymer nanocomposite films were prepared with a gage length, width and thickness of 40 mm 10 mm and 0.28 mm, respectively. Chopped pieces of various casted nanocomposites were filled inside dog-bone shaped cavity of a stainless-steel mould and compression moulded.

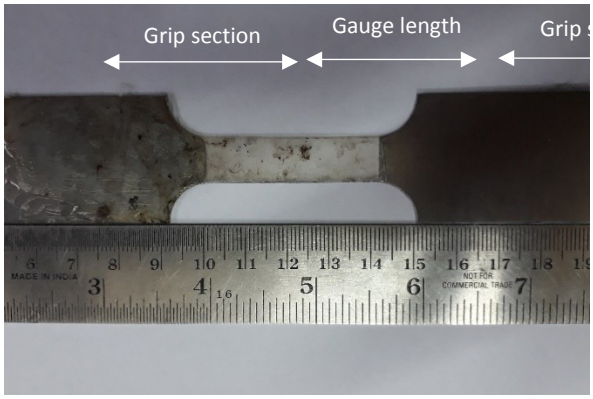


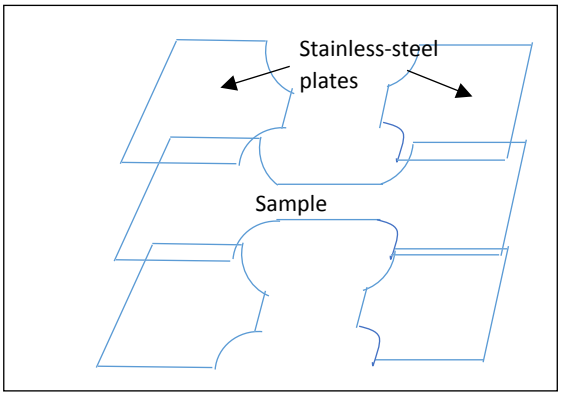


**Figure S1: (a) A tensile sample showing the grip and gage sections. (b) An illustration of the preparation of tensile sample.**

Special effort was given to avoid deformation at the grip section of the dog-bone shaped tensile samples. Four pieces of stainless-steel plates were shaped into the grip section of the tensile sample using electrical discharge machining. These pieces were glued to grip sections of the dog-bone shaped nanocomposite tensile samples from both sides as shown in figure S1 (a) with an illustration in figure S1 (b). Instron mechanical wedge action. grips were used for tensile testing. All nanocomposite samples tested failed in the gage sections.

Speckle patterns were applied in the gage sections of the samples for DIC analysis. Fine black dots (< 100 μm) were sprayed on a white background to make speckle pattern with good contrast on one surface in the gage section. A 2-megapixel camera was placed on a tripod to capture the images while the tests were running. Additional LED lights were installed to get desired brightness as shown in figure S2.

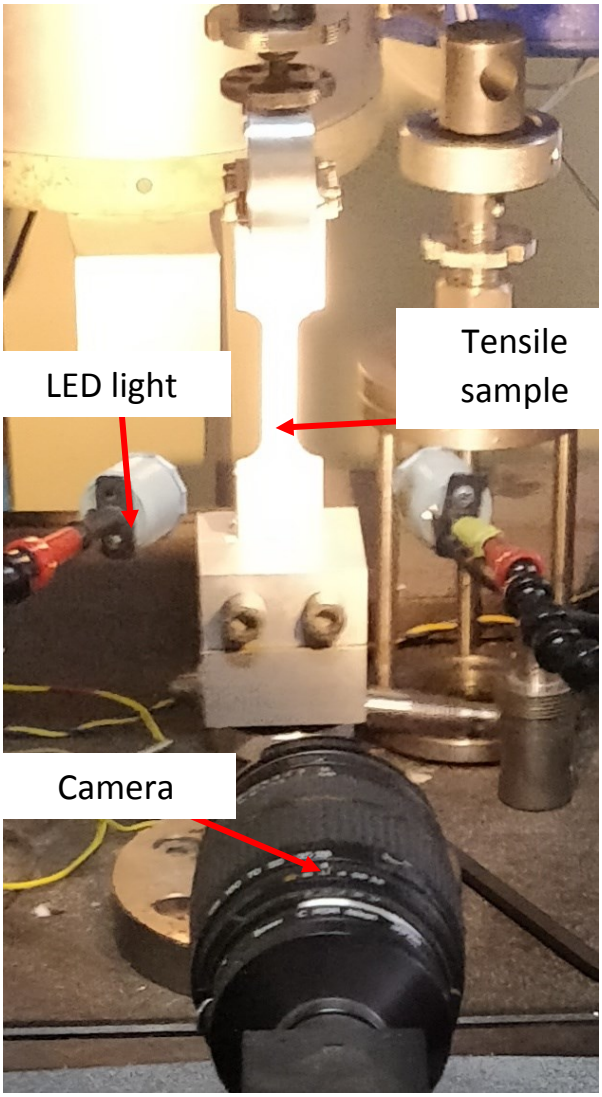


**Figure S2: Mechanical testing unit with an arrangement for DIC. The sample, lights and camera are indicated with red arrows.**

Table T1: Modulus and strength of various PVDF composites.

| Samples | Young's Modulus (MPa) | 0.2% Proof strength (MPa) |
|---|---|---|
| PVDF | 336 | 6.76 |
| PVDF+MWCNT | 472 | 7.36 |
| PVDF+CNS+MWCNT | 524 | 8.11 |
| PVDF+CNS@$SiO_2$+MWCNT | 498 | 8.11 |
| PVDF+CNS@$Fe_3O_4$+MWCNT | 1463 | 24.5 |
| PVDF+CNS@$SiO_2$@ $Fe_3O_4$+CNT | 1492 | 18.5 |

*[Strain rate used : $10^{-4}$ $sec^{-1}$]

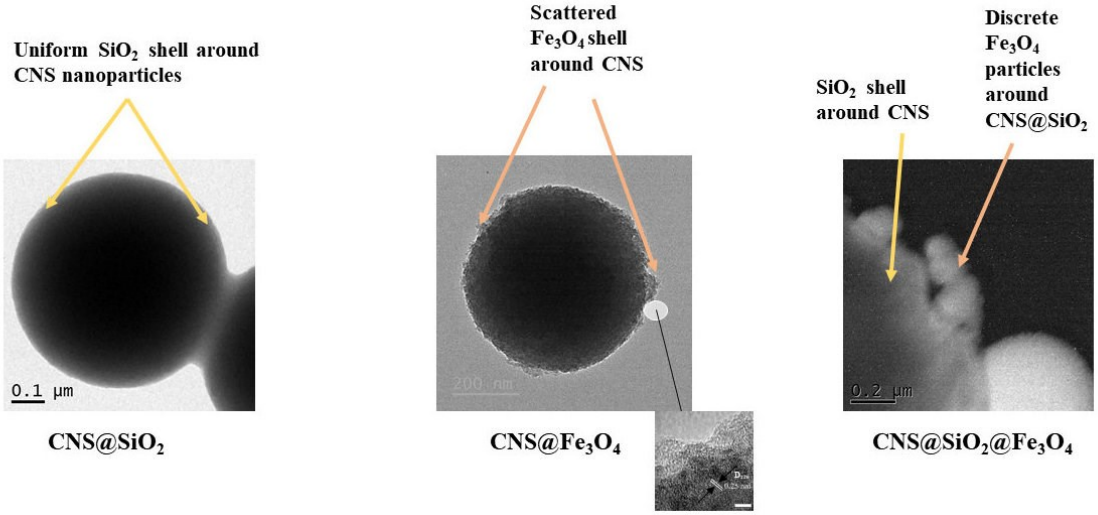


**Figure S3: HR- TEM image of CNS @$SiO_2$, CNS@$Fe_3O_4$ and CNS @$SiO_2$@$Fe_3O_4$. Indicating $SiO_2$ shell layers and discrete $Fe_3O_4$ particle layers. Scale bar denoted in the magnified image is for 5 nm.**

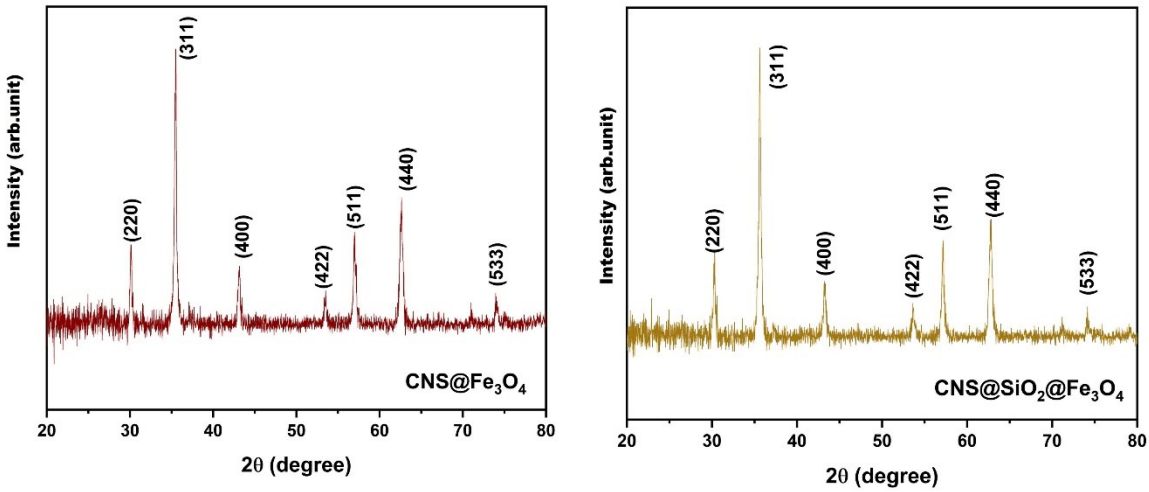


**Figure S4 : Xrd profile for CNS@$Fe_3O_4$ and CNS@$SiO_2$@$Fe_3O_4$**

CNS and $SiO_2$ being amorphous didn't contribute in diffraction pattern, presence of amorphous $SiO_2$ didn't cause much change in peak position, but some small intensity variation was observed in the XRD profile of CNS@$Fe_3O_4$ and CNS @$SiO_2$@$Fe_3O_4$.

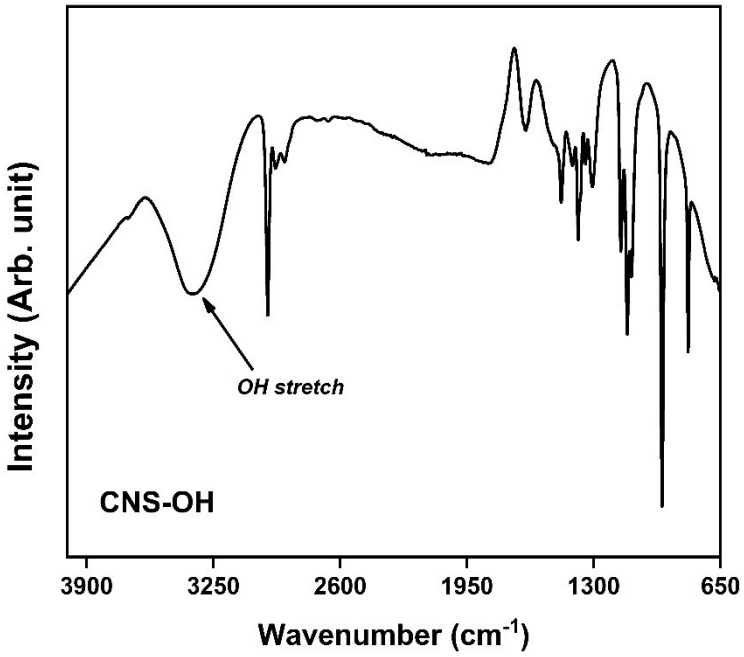


**Figure S5: IR spectrum of hydroxyl functionalised CNS.**

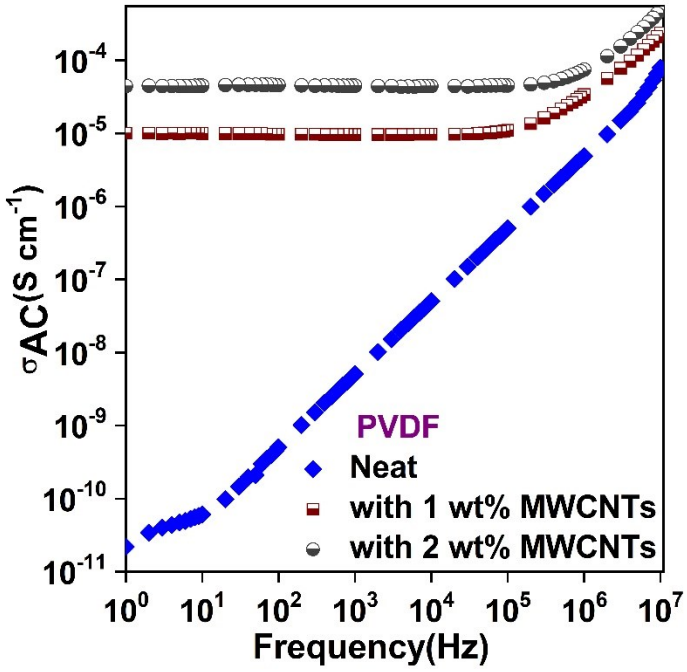


**Figure S6: Conductivity due to variation of MWCNT in the PVDF matrix, below and above percolation threshold with respect to frequency in Hz.**

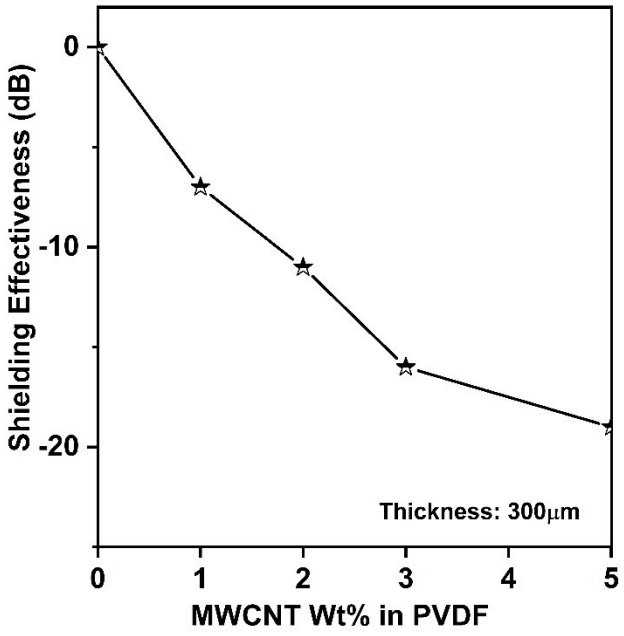


**Fig S7: Shielding effectiveness versus wt% of MWCNT in PVDF**.

MWCNTs were put in PVDF matrix a gradual increase in shielding efficiency with increase in concentration was observed.

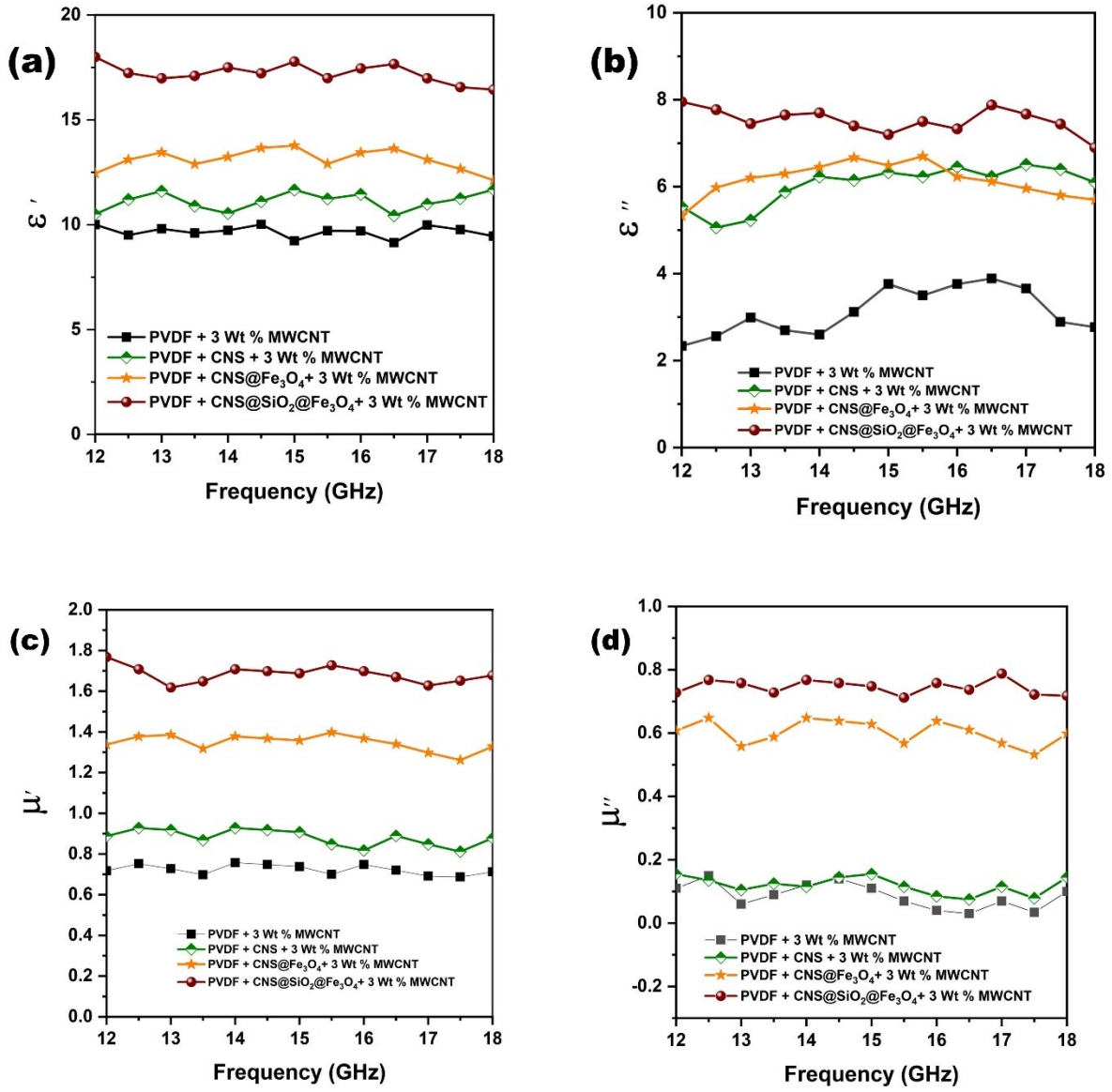


**Figure S8: (a-b) real and imaginary permittivity (c-d) real and imaginary permeability with respect to frequency.**

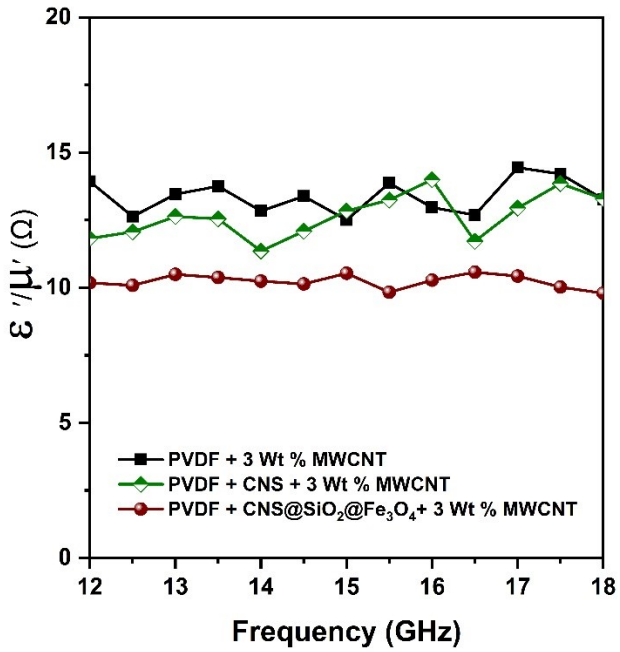


**Figure S9: Impedance matching data. Ratio of real permittivity and permeability.**

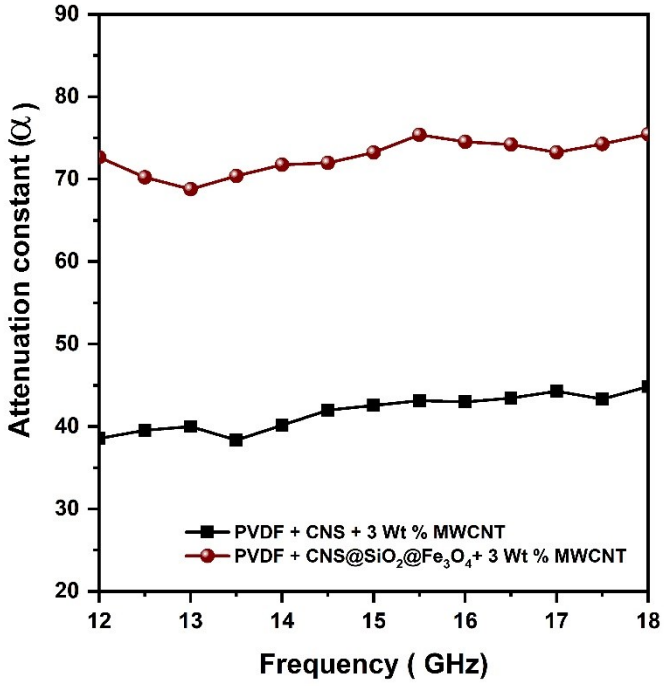


**Figure S10: Graphical representation of attenuation constant.**

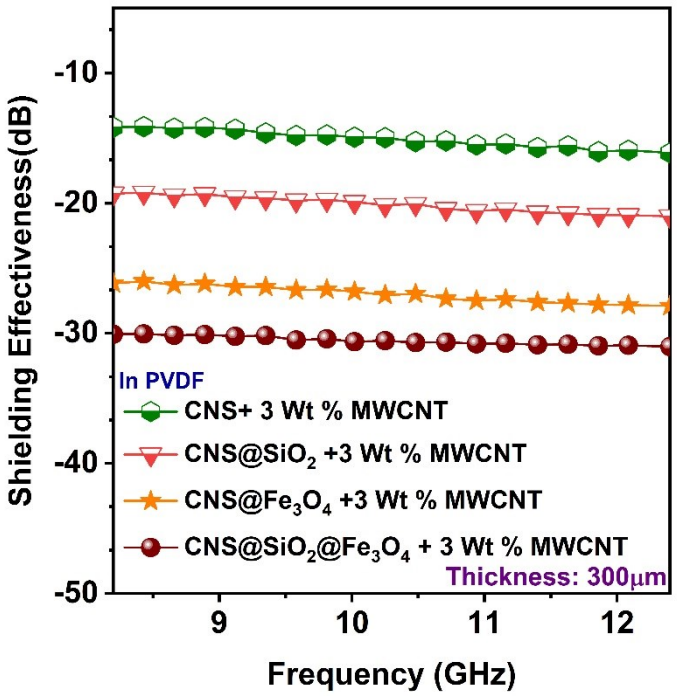


**Figure S11: Shielding effectiveness at X band.**

**Table T2: Table showing various materials available in the market and their shielding values along with the present work.**

| Sl.No. | Materials | EMI SE (dB) | Band |
|---|---|---|---|
| 1. | Metal foils in polymer matrix[1] | 40 | 100-1000 **MHz** |
| 2. | Conductive PAN-nylon cloth[2] | 2 | 100-1000 **MHz** |
| 3. | Ferrite plates[3] | 4 | 100-1000 **MHz** |
| 4. | PVDF core –double shell Heterostructure/MWCNT Composite (This work) | 42 | 12-18 **GHz** |

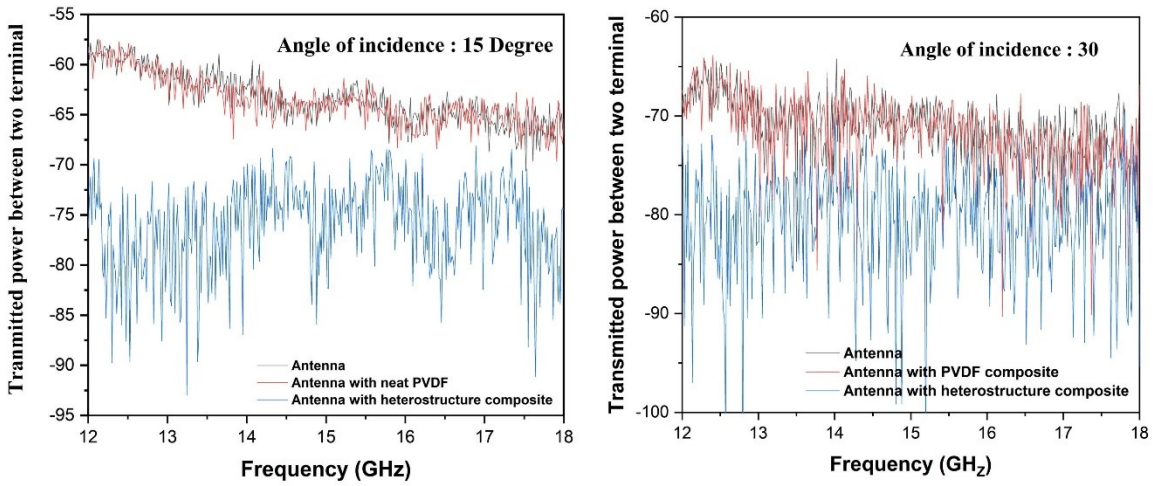


**Figure S12: Transmitted power between two terminal vs Frequency at angle of incidence of 15 and 30 degree.**

CNS heterostrucutre (CNS@$SiO_2$@MWCNT+ 3Wt% MWCNT) composites were used as a shield significant reduction in received power has been observed. This effect is significant in case 0 degree angle of incidence and the received power slowly increases with increased in angle of incidence, which corroborates to the fact that power received without any obstruction and with heterostructure composite are almost same for higher incidence angles (15 and 30 degrees)

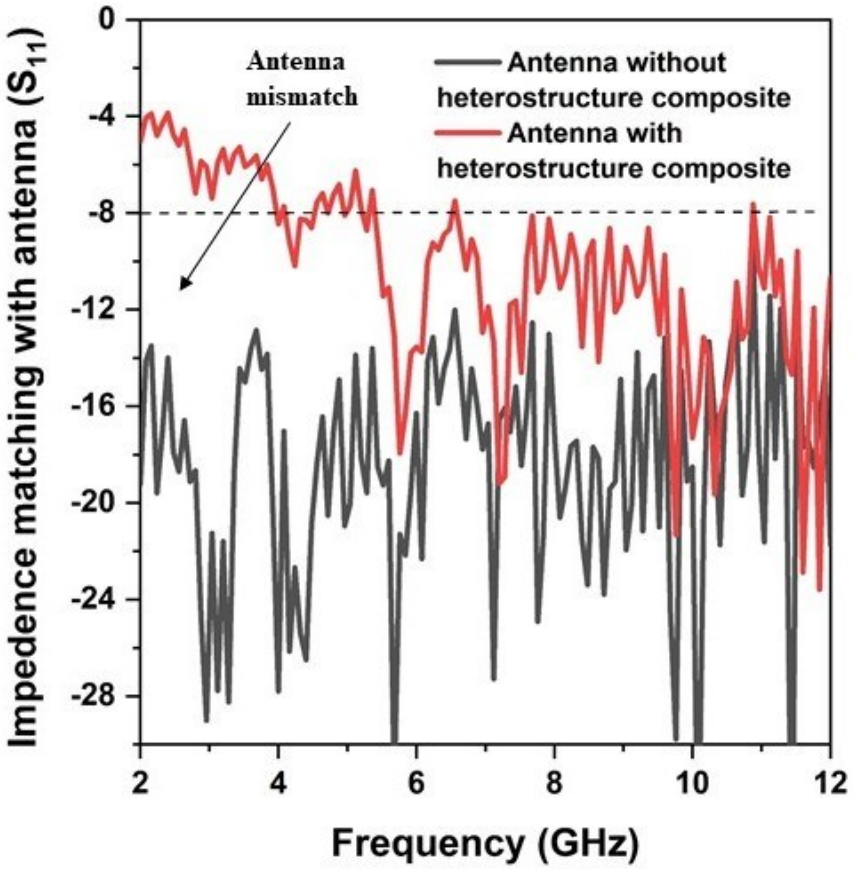


**Figure S13: antenna matching over 2-12 GHz frequency**

Antenna matching is a measure of how much the antenna is radiating at the desired frequency. Eg. -10 dB matching means 10% power is reflected back to the source and 90% is radiated. In antenna engineering -8 to -10 dB matching is usually considered for sufficient performance. For -8 dB matching which means 84% power is radiated efficiently. In our study, we have considered -8 dB as standard. Strong mismatch was indicated in the above figure.

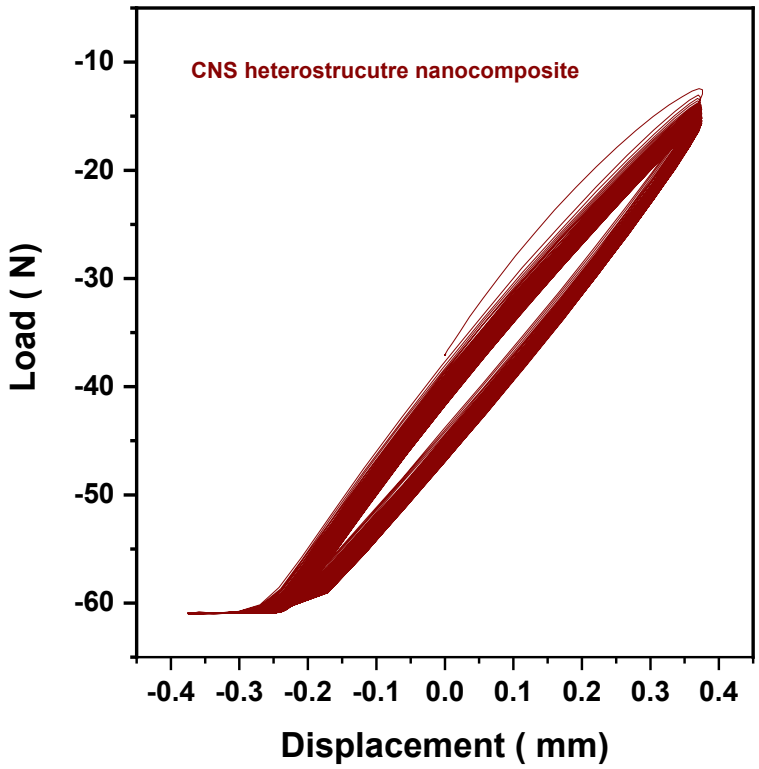


**Fig S14: load vs displacement curve for CNS heterostructure nanocomposites.**

**Reference:**


1. *2009 Wiley Periodicals, Inc. J Appl Polym Sci, 2009*
2. *2009 Wiley Periodicals, Inc. J Appl Polym Sci, 2009*
3. *IEEE TRANSACTIONS ON POWER ELECTRONICS, VOL. 17, NO. 6, NOVEMBER 2002.*